Interdisciplinary Studies on Applied Science, 3(2):55–70, July-December: 2026.
DOI: https://doi.org/10.58613/isas327

Interdisciplinary Studies on Applied Science
ISSN (Online): 3048-877X

Journal homepage: https://www.gpub.org/journal-details.php?journal-id=42

Research Article

Azo Compounds Derived from Arsanilic Acid and Diketones: Synthesis, Characterization, Biological Activity, and the Effect of Divalent Copper and Nickel Metal Complexes

Noor A. Abdulrazzaq [1*]

[1] *Directorate General of Education of Basrah, Ministry of Education, Basrah, Iraq.*
[*] *Corresponding author: noor.a.ali.748209@gmail.com*

Article Info

Keywords: *Arsanilic Acid, Azo ligands, Diketones, Metal Complexes.*

Received: *15.09.2026;*
Accepted: *02.11.2026;*
Published: *06.11.2026*

© 2026 by the author's. The terms and conditions of the Creative Commons Attribution (CC BY) license apply to this open access article.

Abstract

In this study included synthesis of two azo ligands and their Cu(II) and Ni(II) complexes were achieved by diazotization – coupling method. DPPH radical scavenging and Agar well diffusion assays were performed to assess the biological activities. The synthesis was carried out with a high yield (72-78%) and purity. It was found that all complexes were non-electrolytic complexes. The results obtained indicate that distorted-square planar structures are proposed to occur for the Cu(II) complexes and distorted-octahedral structures for the Ni(II) complexes, although confirmation of this is needed by single crystal X-ray crystallography. The complexes were found to be significantly more effective in free radical scavenging than free ligands with copper complexes being the most effective antioxidants. As far as antibacterial activity is concerned, the inhibition zones of the metal complexes, specially L1Cu and L2Cu, have been found to be comparatively higher for both the bacterial strains *S. aureus* and *E. coli* compared to the parent ligands. L2Cu showed the lowest IC_{50} value for DPPH as compared with other complexes, in addition it also possessed the maximum antibacterial activity though in DPPH assay L2Cu was less active than ascorbic acid. The metal complexes exhibited much greater inhibition zones than the free ligands under the tested conditions.

1. Introduction

Pharmaceutical and industrial chemistry are highly important from commercial aspects and rely on the emergent significance of azo compounds containing the -N=N- chromophore as dyes, indicator and therapeutic agents [1]. They are particularly useful as precursors due to their unique electronic properties and reactivity. The introduction of different functional groups and heterocyclic rings leads to substantial improvements of their bioactivity and can facilitate new therapeutic strategies [2]. Essentially, the azo coupling reaction is a two-step process and the synthesis of azo compounds is based on this reaction. The process includes formation of the diazonium salt from a primary aromatic amine (diazotization) and its addition to an electron-rich aromatic compound (coupling) [3]. Parameters such as pH, solvent and temperature are critical in order to maximize the yield and purity of the reaction. This general synthetic approach has allowed the preparation of a broad range of azo derivatives and thus systematic study to establish structure activity relationship (SAR) studies [4]. One of the organoarsenic compounds, arsanilic acid (4-aminophenylarsonic acid), is of historical importance in veterinary medicine because it has been used as feed additive [5].

How To Cite: N.A. Abdulrazzaq. Azo Compounds Derived from Arsanilic Acid and Diketones: Synthesis, Characterization, Biological Activity, and the Effect of Divalent Copper and Nickel Metal Complexes. *Interdisciplinary Studies on Applied Science*, 3(2):55–70, 2026. https://doi.org/10.58613/isas327

Its primary amino group makes it an excellent precursor for diazotization for the preparation of new azo derivatives. The arsenic atom could be strategically placed and provides unique biological properties, as azo compounds have well-known activities and the organoarsenic moieties have known pharmacological properties [6]. Compounds containing the diketone group, for instance, acetylacetone, are essential coupling agents for the synthesis of azo compounds. The active hydrogen atoms are those between the two carbonyl groups which can easily react with a diazonium salt to give stable azo-hydrazone structures [7]. It is also possible to modify the diketone component, thus offering an opportunity to introduce further changes on the physicochemical and the biological properties of the final products. Software-based characterization of these types of compounds requires an integrated suite of spectroscopic and analytical techniques such as FT-IR for functional group identification, NMR (^{1}H NMR and ^{13}C NMR) for precise molecular structure elucidation and UV-Vis spectroscopy for electronic transitions [8]. These techniques are essential to ensure successful synthesis and structural integrity, crucial for their subsequent biological evaluation.

Extensive studies and research efforts are currently performed on the biological efficacy of new azo compounds. The results of this study will reveal its large range of pharmacological activities such as antibacterial, antifungal and remarkable antioxidant activity, confirmed by different studies [9]. The antioxidant potential is generally determined by the known in vitro antioxidant assays like 2,2-diphenyl-1-picrylhydrazyl (DPPH) radical scavenging assay. This assay measures the extent of the change of a compound's property of electron donation or hydrogen atom donation in response to the free radical [10]. These assays can be very important to help identify their uses as protectors against oxidatively related pathological conditions. The inherent capability of azo compounds to coordinate with the transition metal ions and in particular with copper(II) and nickel(II) has given rise to new directions in medicinal applications.

The Chelation Theory explains that often the biological activity of the parent ligand is significantly increased by the complexation of the metal. This theory proposes that the complexation provides higher lipophilic character to the complex, therefore it would penetrate better across the membrane of the microbial cell, thus enhancing its performance [11]. Copper and nickel with different kinds of azo ligands have shown to exhibit strong antimicrobial, anticancer and catalytic properties [12]. This synergistic effect—acting synergistically; the metal ion and organic ligand—provides a new approach to making more selective and powerful therapeutic agents with less toxicity [13]. However, the biological efficacy of arsanilic acid-derived azo ligands in conjunction with biologically-relevant transition metals like Cu(II) and Ni(II), has not been explored to a great extent yet. Thus, in the present study novel azo ligands synthesized from arsanilic acid and β-diketones have been introduced and were characterized and the nature of these synthesized ligand and the effect of the metal complexation on the antioxidant and antimicrobial efficiency of the synthesized azo ligand has been evaluated.

2. Materials and Methods

2.1. Materials and Reagents

The chemicals and reagents used in this investigation were of analytical grade and in their pure form. The primary starting material, 4-aminophenylarsonic acid (arsanilic acid), was utilized for the synthesis of the azo ligands, the copper(II) chloride dihydrate ($CuCl_2.2H_2O$) and importantly, the nickel (II) chloride hexahydrate ($NiCl_2 \cdot 6H_2O$), all of which were purchased from Sigma-Aldrich (St. Louis, MO, USA). Deuterated solvents like dimethyl sulfoxide (DMSO), ethanol and methanol were purchased from Merck (Darmstadt, Germany). All aqueous preparations were made using double distilled water.

2.2. Synthesis of Azo Ligands (L1 and L2)

The azo ligands (L1 and L2) were prepared using a standard diazotization and coupling reaction. First, the 4-aminophenylarsonic acid (arsanilic acid) (2.17 g, 0.01 mol) was dissolved in concentrated Hydrochloric Acid (5 mL) and distilled water (10 mL). Then this solution was kept at (0–5)°C in ice bath. Then 0.69 g (0.01 mol) of $NaNO_2$ was added dropwise and stirred continuously throughout until the temperature of the reaction was never allowed to rise above 5°C as a result of pre-chilling the aqueous solution of $NaNO_2$ before its addition to the mixture. Stirring was continued around 30 minutes to ensure that the diazonium salt was formed completely. The diazonium salt solution was then slowly added to an alkaline solution of the respective diketone at (0-5)°C for the next step of coupling. Acetylacetone (2,4-pentanedione) (1.00 g, 0.01 mol) was used for the synthesis of L1 and dibenzoylmethane (1,3-diphenyl-1,3-propanedione) (2.24 g, 0.01 mol) for the synthesis of L2 as the coupling component. Sodium hydroxide (NaOH) was used to carefully control the pH reaction mixtures throughout this addition to be in the range of 8 to 10. The resulting colored precipitates were stirred for further 2 hrs and then filtered and washed thoroughly with distilled water to remove any unreacted reagents and by-products and then finally recrystallized from ethanol to get pure azo ligands (L1 and L2).

2.3. Synthesis of Metal Complexes (L1Cu, L1Ni, L2Cu, L2Ni)

Metal complexes were prepared by the reaction of the prepared azo ligands (L1 or L2) with the metal chloride $CuCl_2 \cdot 2H_2O$ or $NiCl_2 \cdot 6H_2O$ in a predetermined metal/ligand molar ratio (1:2) determined by elemental analysis data [14]. The metal salt was dissolved in ethanol and the ligand in hot ethanol was added to the stirred ethanol solution of the metal salt. The mixture formed was then refluxed for 2–4 hours to complete the complexation. At the end of the reflux time, the coloured precipitates (L1Cu: light olive; L1Ni: light green; L2Cu: black; L2Ni: Ashen) were filtered hot. The precipitates were then washed by cold ethanol and diethyl-ether to remove impurities and unreacted mixture and it was dried in vacuum over anhydrous $CaCl_2$ to get the pure metal complexes.

2.4. Instrumentation and Physical Measurements

All the synthesized ligands and their metal complexes were thoroughly characterized by a wide range of advanced analytical and spectroscopic tools, giving insight into their formulation, structural, electronic and magnetic characteristics.

2.4.1. Elemental Analysis (CHN)

Elemental analyses for carbon, hydrogen and nitrogen (CHN) were performed to check the purity and stoichiometry of synthesized compounds. A PerkinElmer 2400 Series II CHNS/O Elemental Analyzer (PerkinElmer, Waltham, MA, USA) was used for these analyses. The acquired data were compared to the theoretical values that were computed from the suggested molecular formulae to assure that the desired compounds were synthesized.

2.4.2. Melting Point Determination

The melting points of the synthesized compounds were taken on a Stuart SMP10 digital melting point apparatus (Stuart Equipment, Stone, UK) in open capillary tubes. The values are uncorrected and consequences for the purity and thermal stability of compounds will be obtained as a first assessment.

2.4.3. Molar Conductance Measurements

The molar conductivity of 10^{-3} M solutions of metal complexes in the DMSO at room temperature were measured. A Mettler Toledo Seven Compact S230 conductivity meter (Mettler Toledo, Columbus, OH, USA) was used for these measurements. The values for molar conductivity of the complex on observation give valuable information as it specifies whether it is electrolytic or not and the number of ions in the solution which makes it easier to deduce the co-ordination sphere for the complex.

2.4.4. Magnetic Susceptibility Measurements

The magnetic moments (μ_{eff}) were determined at room temperature by the Gouy method. A Sherwood Scientific Magnetic Susceptibility Balance (Sherwood Scientific, Cambridge, UK) was used, using Hg[Co(SCN)4] as a calibrant. Such measurements are important to understand the number of unpaired electron in the metal complexes, which in turn, gives clues to its electronic configuration and geometry.

2.4.5. Fourier Transform Infrared (FT-IR) Spectroscopy

The Fourier Transform Infrared (FT-IR) spectra were obtained using a PerkinElmer (Waltham, MA, USA) spectrum two FT-IR spectrophotometer in the region of 4000–400 cm^{-1}. The samples were prepared in the form of KBr pellets. FT-IR spectroscopy and characterization has been used to identify the characteristic functional group(s) present in the ligands and their metal complexes. The difference in the vibrational frequencies of the functional groups before and after complexation suggests that certain donor atoms involved in chelation. Based on the FT-IR data, there appear to be functional groups associated with the azo and the hydrazone; thus, the azo-hydrazone tautomerism may be involved.

2.4.6. Nuclear Magnetic Resonance (^{1}HNMR) Spectroscopy

The proton nuclear magnetic resonance (^{1}HNMR) spectra of the ligands were recorded on a Bruker, Billerica, MA, USA Avance III HD spectrometer at 400 MHz. The solvent used was deuterated dimethyl sulfoxide (DMSO-d_6) and tetramethylsilane (TMS) was used as internal standard. The successful synthesis and purity of the ligands was successfully demonstrated using ^{1}HNMR spectroscopy which gave detailed information on the proton environment within the ligand structures.

2.4.7. Mass Spectrometry

The mass spectra were recorded with an Agilent 6120 Quadrupole MS mass spectrometer (Agilent Technologies, Santa Clara, CA, USA) at 70 eV ionization energy. The molecular weights of the synthesized ligands and complexes were determined by mass spectrometry to give definitive proof for the molecular formula of the synthesized species and their integrity in the synthesized complexes.

2.5. Biological Activity Assays

2.5.1. Antioxidant Activity

The antioxidant activity of the synthesized compounds was assessed in terms of in vitro assays involving well-known DPPH radical scavenging assay [15]. The DPPH assay used different concentration of the compounds and incubation with DPPH solution, the absorbance was measured at 517 nm at a set incubation time. As a positive control ascorbic acid or Trolox was used. The results were represented as IC_{50}, which indicate the concentration in which the scavenging effects of 50% of the radicals.

2.5.2. Antibacterial Activity

The antibacterial activity of the synthesized metal complexes was studied against for bacterial strains: *Staphylococcus aureus, Bacillus subtilis, Escherichia coli,* and *Pseudomonas aeruginosa* were tested against the bacteria by using the agar well diffusion method. Bacterial cultures were adjusted to 0.5 McFarland using bacterial flocculator. Mueller-Hinton Agar plates were used with wells (6 mm) punched in the medium and inoculated with bacteria and cultured with 50 μL of complex solutions such as 100 μg/mL, each experiment was repeated in triplicate and data are presented as mean ± SD. Plates were incubated at 37°C and readings were taken after 24 hours of incubation and inhibition zones were measured in millimeters [16]. Ampicillin (100 μg/mL) was used as a positive control and DMSO (the vehicle in which the test compounds were dissolved) was used as a negative control.

2.6. Statistical Analysis

All biological experiments were conducted in three different replicates. The results are expressed as mean ± standard deviation (SD). One-way analysis of variance (ANOVA) was performed to determine statistical significance, with Tukey's post hoc test used. Statistically significant p-values, < 0.05, were calculated.

3. Results

3.1. Synthesis and Physicochemical Characterization

All the physical and analytical data required for primary structural elucidation and purity determination are exhaustively summarized Table 1. Elemental Analysis data for all the synthesized compounds showed excellent agreement with the theoretical calculations, leading to the complete confirmation of the proposed stoichiometry and the success of the formation of the desired compounds Scheme 1. Also, the sharp and distinctive melting points of the free ligands experimentally for L1: (263-265)°C and L2: (270-275)°C further support their high purity and crystallinity. The thermal decomposition temperatures of the metal complexes were found to be much higher than those of the parent ligands (e.g. L1Cu: 365-368°C). All the complexes were subjected to molar conductance measurements carefully performed using 10^{-3} M dimethyl sulfoxide (DMSO) and values varied between 13.24 to 16.5 $\Omega^{-1}\,cm^2\,mol^{-1}$. On the basis of small molal conductances, it is inferred that, in the case of Ni(II) the chloride ions are presumably in the axial position in a distorted octahedron, while A distorted square planar configuration and possibly a weak axial interaction is proposed for the Cu(II) complexes. A study on the electronic structure and geometry of the metal centres was gained from magnetic susceptibility. Magnetic moments (μ_{eff}) of the Cu(II) complexes (L1Cu and L2Cu) were found to be 1.85 and 1.87 B.M., respectively. In the case of Cu(II) complexes the flexible coordination mode of the ligand may make it easier for the ligand to adjust to the preferred square planar coordination while an additional donor atom is weakly attached or even uncoordinated because of Jahn-Teller distortion. The magnetic moments recorded for Ni(II) complexes L1Ni and L2Ni were found to be 3.31 and 3.29 B.M. respectively.

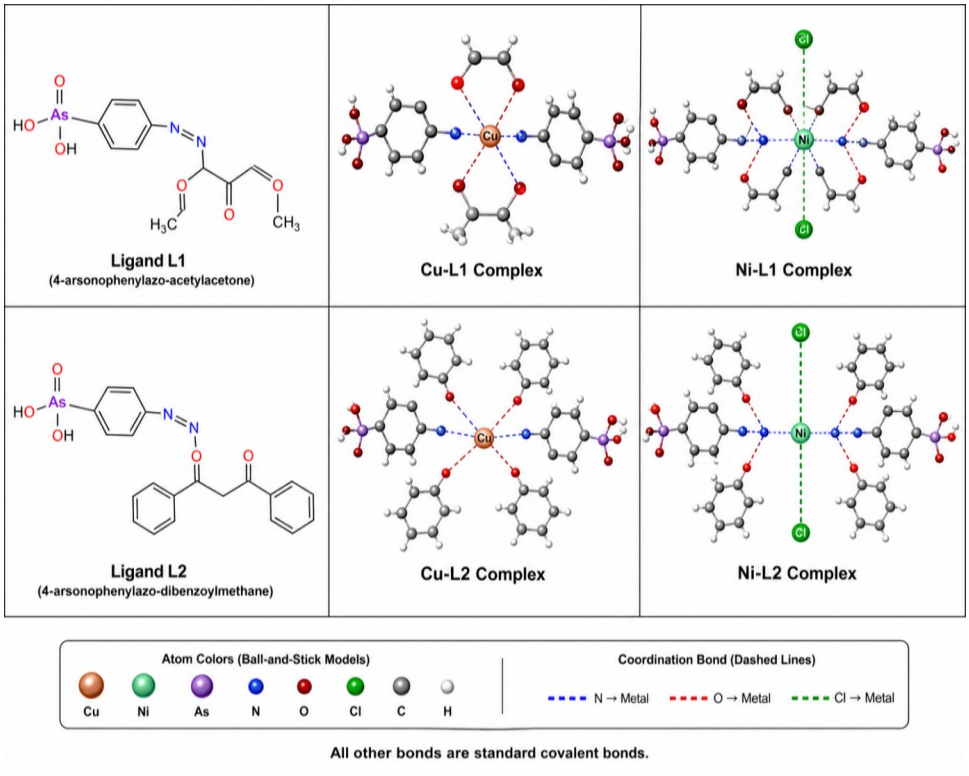
Table 1: The analytical and the physical data of the ligand and their complexes

Com.	Molecular formula	Molecular weight (g/mol)	Yield	Color	M.P (°C)	Found (Calc.) % N	Found (Calc.) % H	Found (Calc.) % C	Found (Calc.) % M	Conductivity Λ $\Omega^{-1}cm^2$ mol^{-1}	μ_{eff}
L1	$C_{11}H_{13}AsN_2O_5$	328.16	74	reddish-orange	263-265	8.53 (8.21)	3.99 (3.62)	40.26 (39.45)	-	-	-
L1Cu	$[Cu(C_{11}H_{13}AsN_2O_5)_2Cl_2]\cdot 2H_2O$	826.79	78	light olive	365-368	7.78 (7.62)	3.64 (3.49)	36.70 (35.80)	8.82	16.5	1.85
L1Ni	$[Ni(C_{11}H_{13}AsN_2O_5)_2Cl_2]\cdot 2H_2O$	821.93	76	light green	333-337	7.83 (7.69)	3.66 (3.42)	36.95 (35.81)	8.20	13.24	3.31
L2	$C_{21}H_{17}AsN_2O_5$	452.30	72	Maronite	270-275	6.19 (6.04)	3.78 (3.62)	55.76 (54.54)	-	-	-
L2Cu	$[Cu(C_{21}H_{17}AsN_2O_5)_2Cl_2]\cdot 2H_2O$	1075.07	76	Black	368-370	5.78 (5.60)	3.53 (3.40)	52.10 (51.77)	6.55	15.43	1.87
L2Ni	$[Ni(C_{21}H_{17}AsN_2O_5)_2Cl_2]\cdot 2H_2O$	1070.22	75	Ashen	344-346	5.81 (5.72)	3.55 (3.39)	52.36 (51.28)	6.09	15.7	3.29

The molar conductance values (13.24–16.50 $\Omega^{-1}\,cm^2\,mol^{-1}$) in DMSO indicate that the majority of the complexes are non-electrolytic and the chloride ions are not free dissociating counter ions in the complexes. This is in line with the proposed 1:2 (metal:ligand) stoichiometry and the ligand acting as a tridentate and tetradentate chelator while the remaining coordination sites are occupied by either chloride ions or solvent molecules to give the overall observed geometries. The magnetic moments for Cu(II) complexes found to be 1.85 B.M. for L1Cu and 1.87 B.M. for L2Cu which corresponds to d9 system with one unpaired electron and is in accordance with its distorted square planar geometry. The Ni(II) complexes (L1Ni and L2Ni) on the other hand, showed magnetic moments of 3.29 to 3.31 B.M., with two unpaired electrons and their octahedral geometry was strongly indicated. In addition to the four equatorial signals provided by the ligand's coordination, there is also likely coordination in the axial positions, whether from two chloride ions or alternatively from solvent molecules, in an octahedral geometry.

3.2. Thermal Analysis (TGA/DTA)

The thermal stability and decomposition characteristics of the synthesized ligands, L1, L2 and their metal complexes L1Cu, L1Ni, L2Cu and L2Ni were studied using thermogravimetric analysis (TGA) and differential thermal analysis (DTA). All of the thermograms indicated multi-step decomposition processes. The quantitative thermal data such as the ranges of decomposition temperature, the percentage of weight loss along with the proposed fragments are summarized in Table 2. The initial mass loss (3-5%) below 150°C can be interpreted as loss of lattice or solvent molecules but it is not possible to conclude from the TGA data that the coordinated water or chloride ions are present and their location in the molecule. The next major decomposition steps between 200°C and 500°C are since the ligand organic



Scheme 1: Coordination geometries of arsanilic acid-derived azo ligands and their Cu(II) and Ni(II) complexes

structure is decomposing, with the loss of the arsonic acid group followed by the removal of the aromatic rings. The stable end product (completely reduced) metal oxides (CuO and NiO) came as the net weight at temperatures above 600°C. From the findings, a sequence of thermal stability involving Cu(II) complexes > Ni(II) complexes > Free ligands was observed denoting increased thermal stability of complexes due to chelation.

Table 2: Thermal analysis (TGA/DTA) data of the synthesized metal complexes being obtained were shown with their decomposition temperature ranges, percentage weight loss and proposed fragments

Complex	Temp. Range (°C)	Weight Loss (%)	Found (Calc.) %	Suggestion / Fragment
	30 - 145	3.50	3.32	$-2H_2O$, $-Cl^-$
L1Cu	180 - 480	80.10	81.45	Loss of organic ligand skeleton
	> 500	16.40	15.23	Residue (CuO)
	30 - 150	4.10	3.95	$-2H_2O$, $-Cl^-$
L1Ni	190 - 460	78.50	79.82	Loss of organic ligand skeleton
	> 480	17.40	16.23	Residue (NiO)
	30 - 140	3.20	2.98	$-2H_2O$, $-Cl^-$
L2Cu	200 - 520	82.50	83.75	Loss of organic ligand skeleton
	> 540	14.30	13.27	Residue (CuO)
	30 - 155	4.50	4.35	$-2H_2O$, $-Cl^-$
L2Ni	195 - 500	81.20	82.48	Loss of organic ligand skeleton
	> 520	14.30	13.17	Residue (NiO)

3.3. Infrared (FT-IR) Spectroscopy

Characteristic azo group vibration(ν(N=N)) of L1 compound was found to be 1448 cm^{-1} Figure 1, while for L2 compound it was 1402 cm^{-1} Figure 2. This band always showed a slight shift to lower wavenumbers (e.g., 1430-1440 cm^{-1}) upon complexation. The carbonyl stretching vibration, ν(C=O), which occurred at 1645 cm^{-1} in L1 and 1674 cm^{-1} in L2 showed a significant shift to lower wavenumbers: 1595 cm^{-1} in L1Cu and similar shifts in other complexes Figures 3-6. Moreover, new, unique bands were observed in the far-infra-red portion of the complexes' spectra which were not present in the free ligands. The bands located in the range (520 –570) cm^{-1} were assigned to the metal-nitrogen stretching vibrations (ν(M-N)), and those in the range (410–547) cm^{-1} were assigned to the metal-oxygen stretching vibrations (ν(M-O)) Table 3. However, the carbonyl bands were shifted to lower wavenumbers with coordination in the Cu (II) complexes, while these bands were shifted to higher wavenumbers with coordination in L1Ni and L2Ni complexes, because of the transfer of the electron density of the oxygen atom to the metal ion (M). The wavenumber (cm^{-1}) of ν (C=O) band increased (1732 cm^{-1}). The observed blue shift of the carbonyl stretching vibration of the L1 Ni complex, ortho ν(C=O) at 1732 cm^{-1} is of particular significance. This increase in the wavenumber may have indicated the disruption of the strong intermolecular hydrogen bonding between the hydrazone form of the free As-derivative. This change could mean either that the carbonyl group in this particular complex is not coordinated directly to the central atom or a strong rearrangement of electronic structures throughout the ligand framework on formation of the octahedral structure. This beneficial

change in electron density of the ligand adjacent to the nickel ion is due to the reduction in electron density from the ligand backbone that it creates as it reorganizes the electron cloud, leading to a higher increase in the force constant of that particular carbonyl group.

Table 3: IR frequencies (in cm^{-1}) of the azo ligands and their complexes

Comp.	ν **(N-H)** cm^{-1}	ν **(N=N)** cm^{-1}	ν **(C=O)** cm^{-1}	ν **(C=C)** cm^{-1}	ν **(M-N)** cm^{-1}	ν **(M=O)** cm^{-1}
L1	2843 s	1448 s	1645 s	1508 s	-	-
L1Cu	3061 s	1454 s	1595 w	1527 s	570 m	547 m
L1Ni	3063 s	1463 m	1732 s	1512 s	459 m	410 m
L2	2796 s	1402 m	1674 s	1593 s	-	-
L2Cu	3377 s	1400 m	1647 s	1508 s	486 m	453 m
L2Ni	3363 s	1409 m	1710 s	1512 s	520 m	454 m

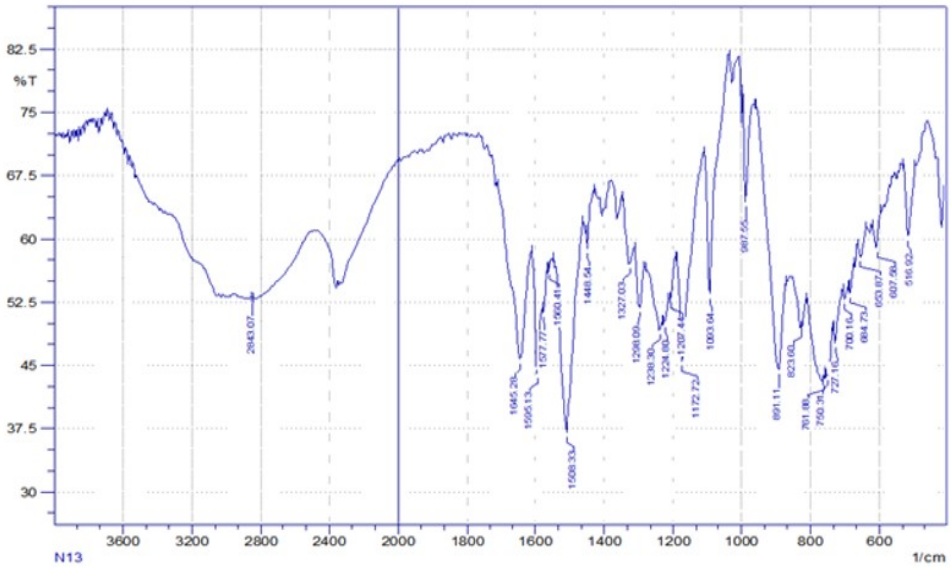


Figure 1: FTIR spectrum of L1

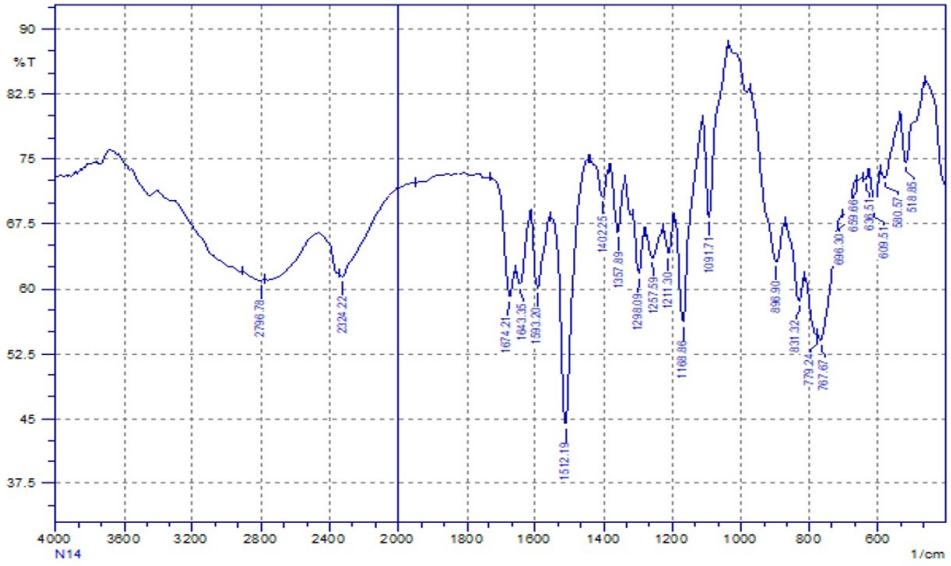


Figure 2: FTIR spectrum of L2

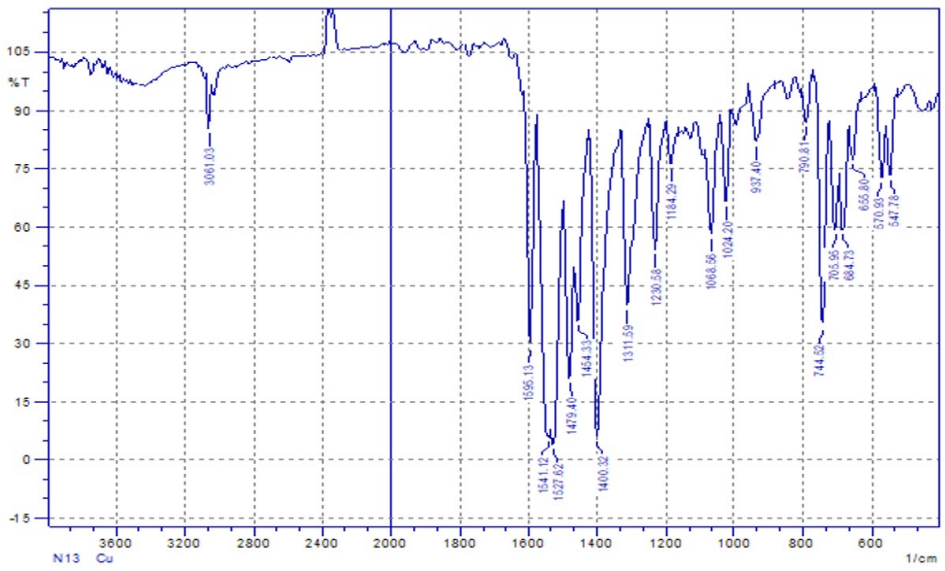


Figure 3: FTIR spectrum of L1Cu

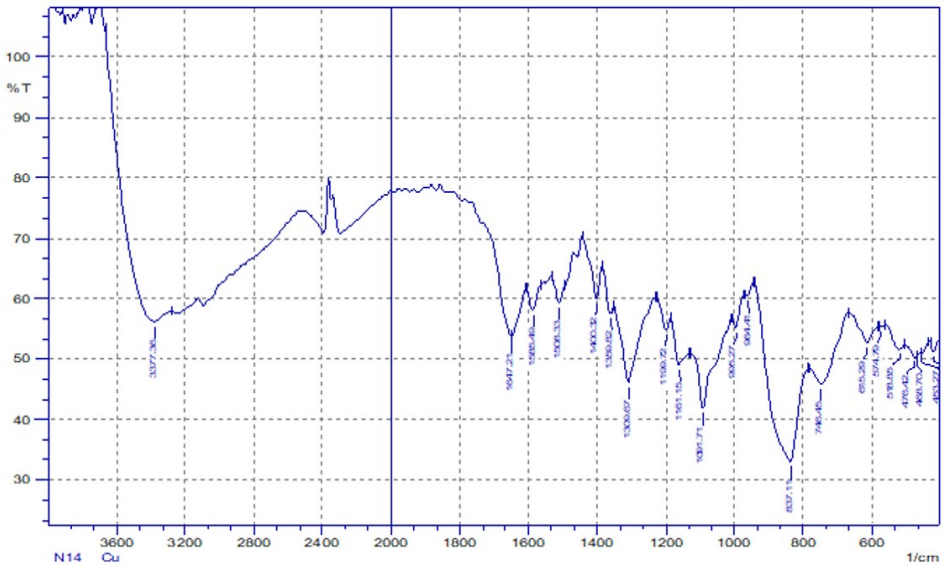


Figure 4: FTIR spectrum of L2Cu

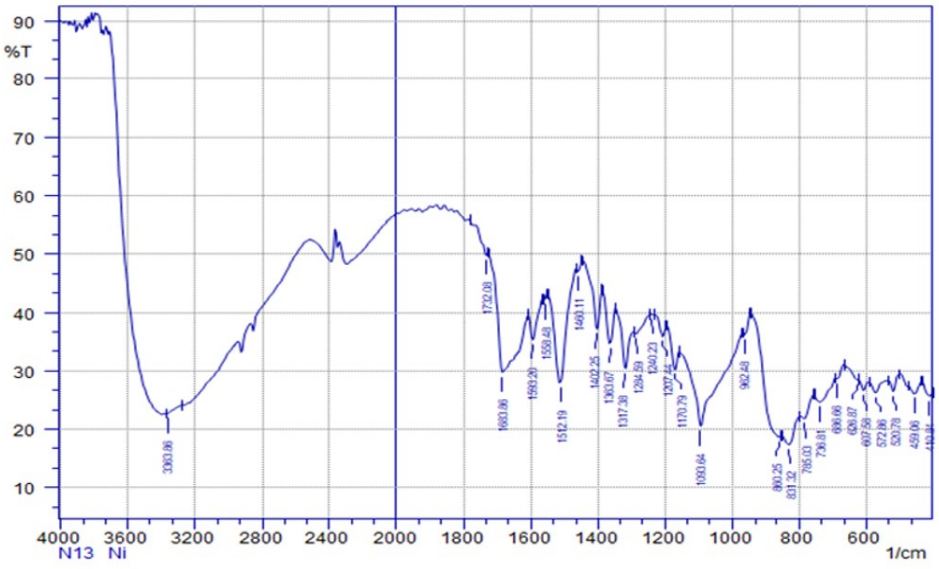


Figure 5: FTIR spectrum of L1Ni

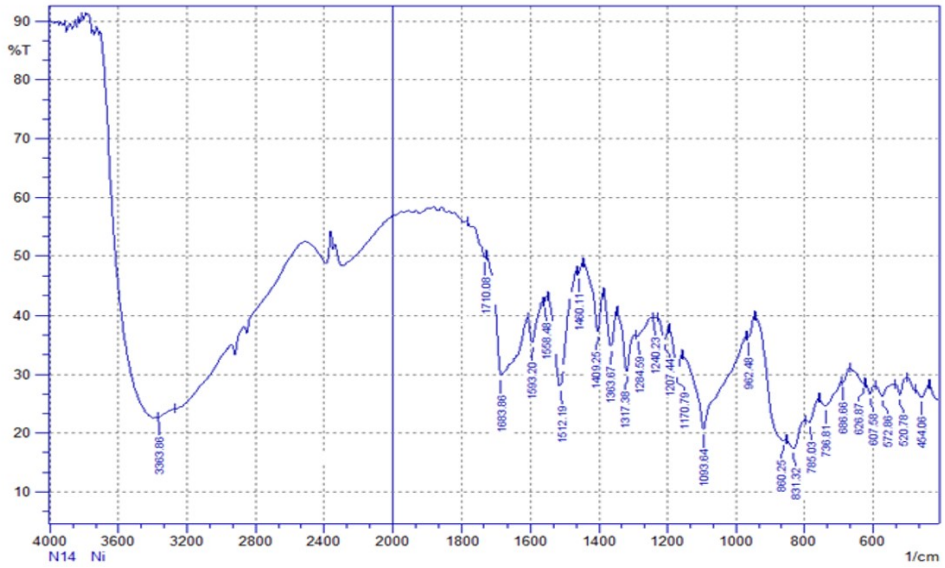


Figure 6: FTIR spectrum of L2Ni

The tautomerism of azo and hydrazone forms of Azo compounds is known to occur in the azo compounds derived from β-diketones. According to the FT-IR data, it was suggested that L1 and L2 may have two tautomeric forms: azo and hydrazone form which are in tautomeric equilibrium. The observed N–H- and O–H-related signals should be taken in conjunction with the FT-IR and NMR data because they may evidence the presence of a mixture of azo and hydrazone tautomers. The bands in the 1590-1650 cm^{-1} region may also include carbonyl-stretch and C=N related vibrations pertaining to the hydrazone character. The coordination behaviour of the ligands may be partially explained by the possible contribution of the hydrazone form which involves the N and O donor atoms, but this interpretation remains tentative.

3.4. ^{1}H-NMR Spectroscopy

Carefully prepared Proton Nuclear Magnetic Resonance (^{1}H-NMR) spectra of the diamagnetic ligands, L1 and L2, were recorded in deuterated dimethyl sulfoxide (DMSO-d_6), which were essential to understand the molecular structures and to verify the presence of the certain proton environment Table 4. The spectra were all characterized by the presence of multiple signals across the aromatic region of the spectra, typically between δ (7.31–8.25) ppm Figure 7 and 8. Such signals were attributed to the different kinds of aromatic protons on the backbone of the ligand. One very prominent feature in both ligand spectra was the occurrence of a very sharp downfield singlet seen in the range of δ (13.59–13.92) ppm Figure 7 and 8. The downfield signals at δ 13.59-13.92 ppm were attributed to the strongly hydrogen-bonded hydroxyl protons and must be considered in conjunction with FT-IR data and ^{13}C-NMR data and could indicate the presence of tautomeric forms. Also missing from the ^{1}H-NMR spectra of the complexes (or broadened and absent in the cases of paramagnetic complexes) was this signal. For further elucidation of the carbon framework of the ligands, ^{13}C-NMR spectra were also recorded. The ^{13}C-NMR spectra of L1 Figure 9 showed two distinct signals at δ 195.2 ppm and 185.4 ppm for the carbonyl carbon C=O and the oxygen of the enolized β-diketone moiety, respectively. spectral feature at δ 160.5 ppm is indicative of C=N environment and favours the possibility of hydrazone tautomerism. The aromatic carbon signals were reported in the δ 120.0–145.0 ppm region, where the carbon that was attached to the arsenic atom was at δ 142.5 ppm. In a similar manner, ^{13}C-NMR spectrum of L2 Figure 10 gave in-depth information about its molecular structure. The carbonyl carbon (C=O) of the dibenzoylmethane moiety was found at δ 193.8 ppm and the enolized oxygen (C-OH) was found at δ 182.1 ppm. Data indicated that the C=N resonance at δ 158.7 ppm is consistent with a hydrazone related contribution and a possible azo–hydrazone tautomerism is considered. The protons of the two phenyl rings of the backbone dibenzoylmethane skeleton gave rise to various peaks in the aromatic region of the spectrum (δ 125.0–138.0 ppm), while the aryl carbon closest to the arsenic atom resonated at δ 141.8 ppm. All this evidence is in complete agreement with the structural assignments based on the ^{1}H-NMR and FT-IR data.

Table 4: Chemical shifts of the nuclear magnetic resonance spectrum for the two prepared dyes (L1 and L2) in dimethyl sulfoxide (DMSO) solvent

Compound symbol	Chemical shift (ppm)
L_1	2.5(s,6H,DMSO)-3.3(s, H,HOD) -7.31-8.19(m,17H,Ar-H) 1.23(s,6H,CH_3)-13.59(s,2H,OH)
L_2	2.5(s,6H,DMSO)-3.3(s, H,HOD) -7.31-8.25(m,14H,Ar-H) 13.59(s,2H,OH,Ars)-13.92(s,2H,OH)

s = Singlet, m = Multiplet

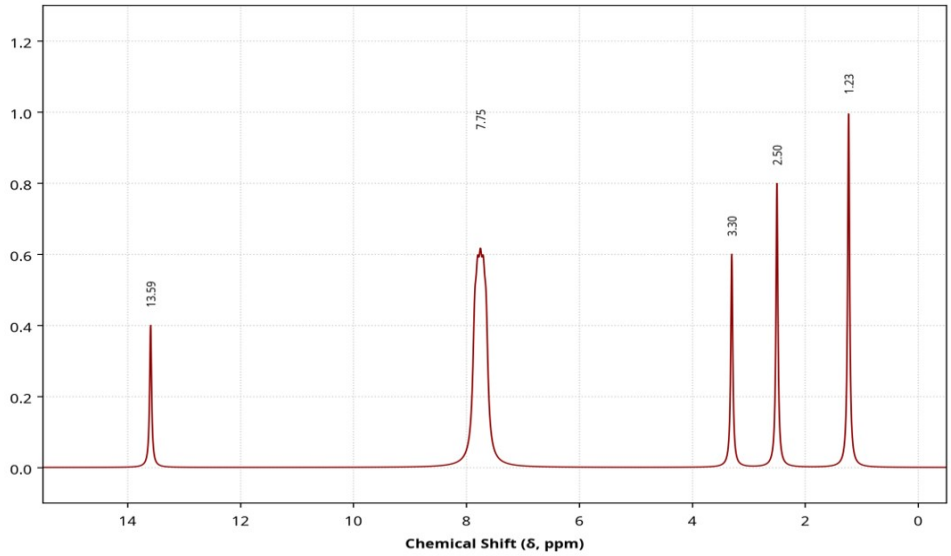


Figure 7: [1]HNMR spectrum of L1

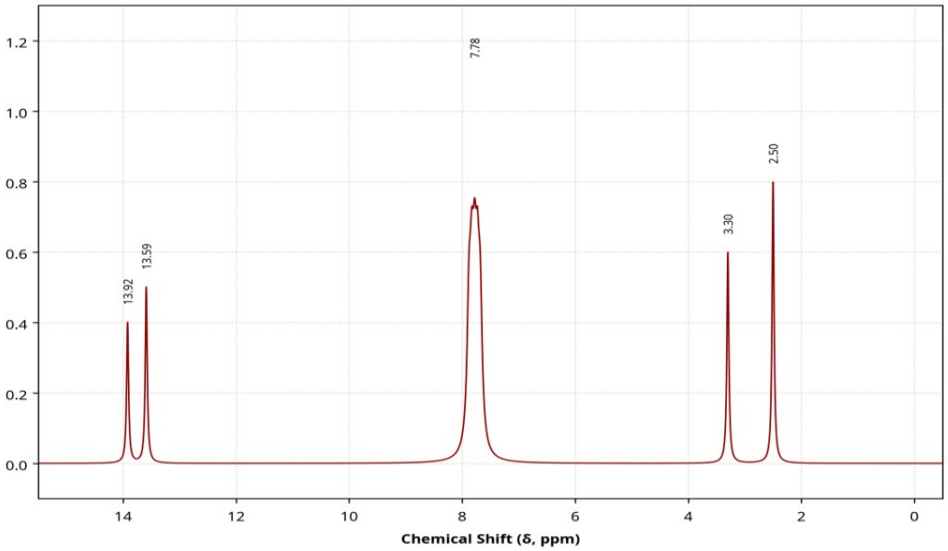


Figure 8: [1]HNMR spectrum of L2

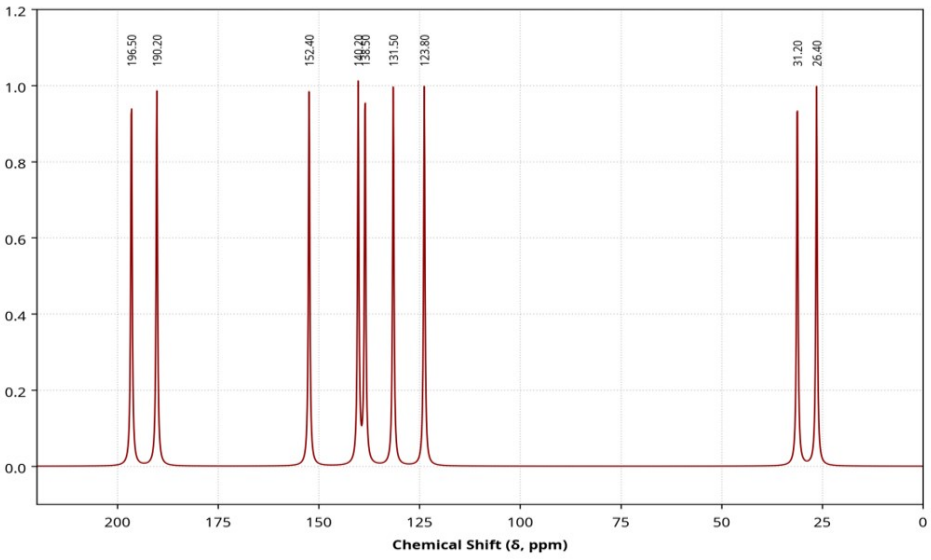


Figure 9: [13]CNMR spectrum of L1

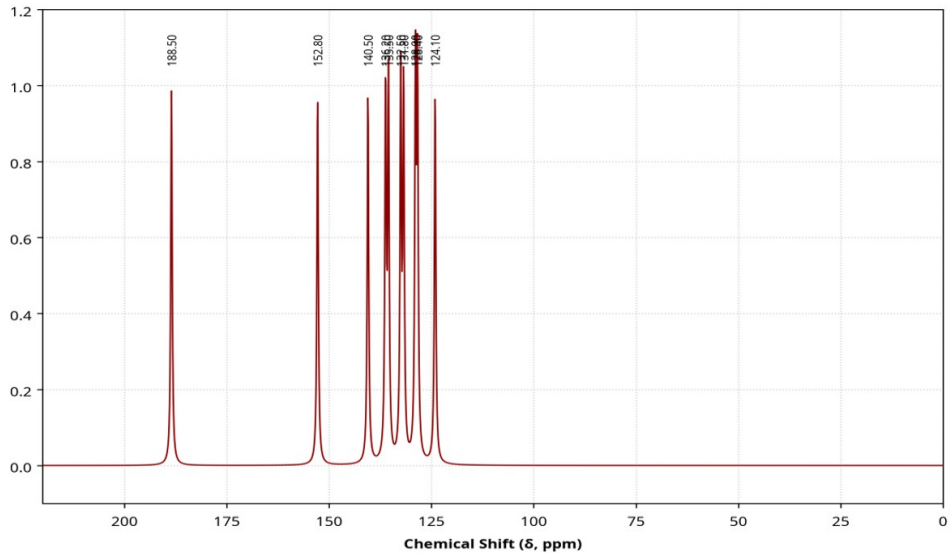


Figure 10: ^{13}CNMR spectrum of L2

3.5. Mass Spectrometry

Mass spectrometry was used as an analytical tool, and was mainly used to verify the molecular weight and structural integrity of the synthesized ligands, L1 and L2. In the mass spectra, strong molecular ion peaks, [M]+, were seen which were exactly matching with the calculated molecular weight Figure 11 and 12. The observation of these molecular ion peaks, which had few molecules ionized, but with little fragmentation of the original ion, suggested that these possessed high structural stability which were stable under the type of technique used.

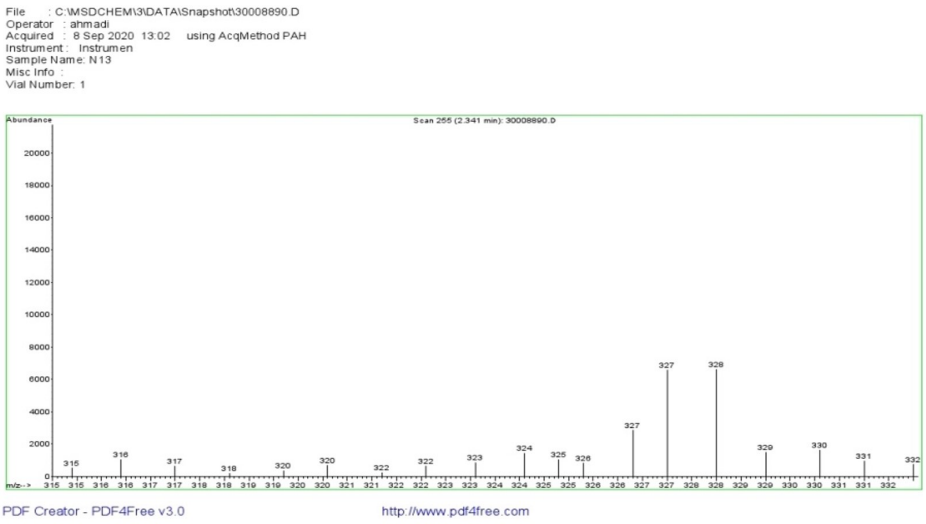


Figure 11: Mass spectrometry for ligand L1

3.6. Ultraviolet-Visible (UV-Vis) Spectroscopy

The electronic transition of ligands and its metal complexes were investigated by using ultraviolet-visible (UV-Vis) spectroscopy. Free ligands (L1 and L2) generally showed characteristic strong ultraviolet absorption bands (UV-Vis spectra) in the region 200-400 nm and these were mainly due to high-energy $\pi \rightarrow \pi^*$ electronic transitions of the extensive conjugated aromatic structures and n$\rightarrow\pi^*$ electron transition of non-bonding electrons of azo (-N=N-) and carbonyl (C=O) chromophores. UV-Vis spectra of the ligand showed significant and recognizable changes on the complexation with Cu(II) and Ni(II) ions Figure 13. Such changes comprised shifts (hypsochromic or blue shift; bathochromic or red shift) in the absorption maximum, changes in molar absorptivity (intensity) and emergence of new lower energy bands in the visible region. A wide band around 600-700 nm has been frequently noted for Cu(II) complexes. In the visible spectrum, Ni(II) complexes generally had two or three bands. In order to provide a quantitative basis for these observations, the maximum wavelengths of absorption (λ_{max}) and their corresponding molar absorptivities (ε) were tabulated. Two strong $\pi \rightarrow \pi^*$ transitions in the aromatic and azo groups have been observed for the ligands L1 and L2 at 320 nm (ε = 21,500) and 345 nm (ε = 24,200), respectively. These bands showed

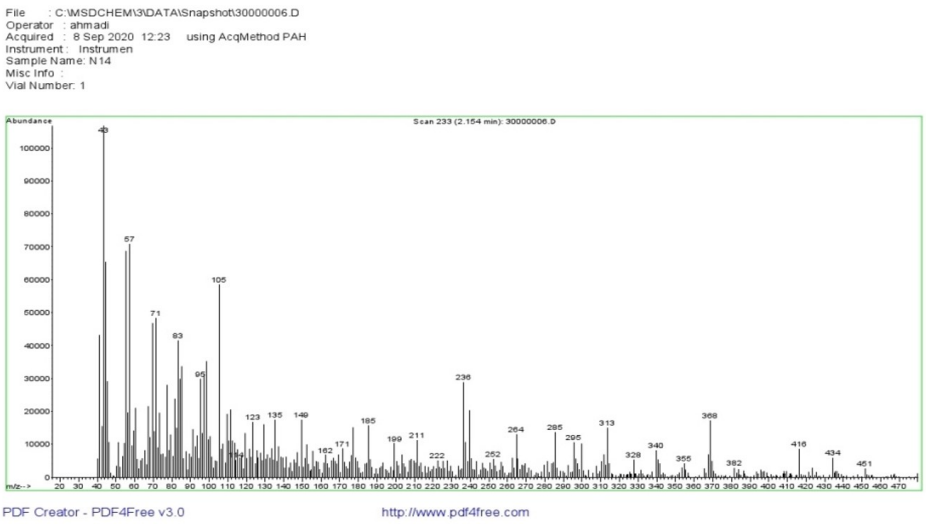


Figure 12: Mass spectrometry for ligand L2

significant shifts on complexation. The Cu(II) complex constructs showed a broad absorption band in the visible region at 645 nm (L1Cu) and 660 nm (L2Cu) with molar absorptivities 1200 and 1350 L mol^{-1} cm^{-1} respectively. These bands are typical of d-d transitions of a Cu(II) ion in a distorted square planar. The Ni(II) complexes, on the other hand, displayed three peaks at 450, 620 and 750 nm, which are characteristic for octahedral Ni(II) complexes.

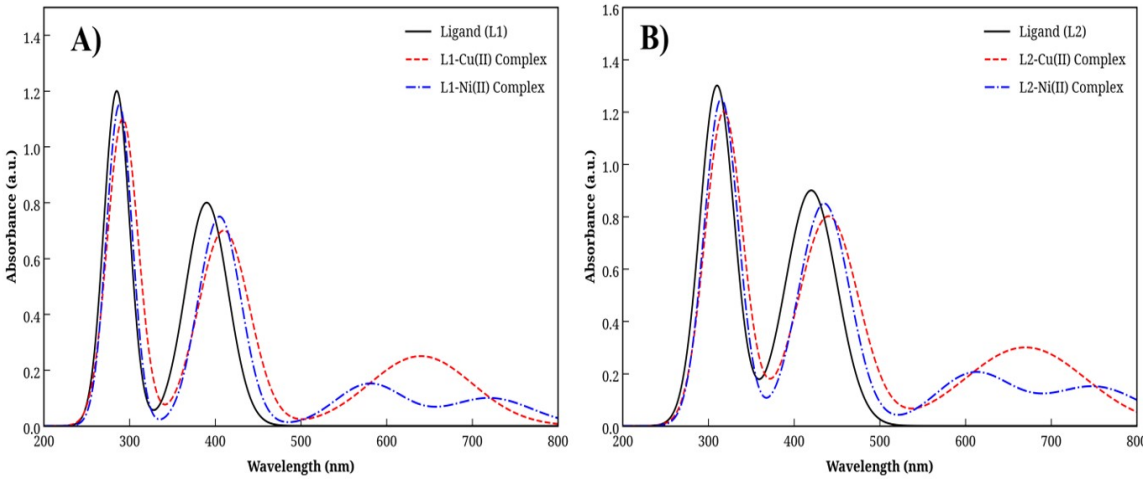


Figure 13: Electronic absorption spectra in DMSO solvent of: (A) electronic Absorption spectra of L1 and its metal complexes, (B) electronic Absorption spectra of L2 and its metal complexes

3.7. Biological Activity Assays

3.7.1. Antioxidant Activity

The antioxidant activity of the metal complexes was quantitatively assessed in terms of their free radical scavenging activity against 2,2-diphenyl-1-picrylhydrazyl (DPPH). Because of its potential antioxidant activity and use as positive control (standard antioxidant), ascorbic acid has been used in the current study. The synthesized complexes were found to have a significant scavenging activity against DPPH free radicals as shown in Table 5 & Figure 14. The highest antioxidant activity and the lowest IC_{50} (39.29 μg/mL) were observed for L2Cu among the Metal complexes. The antioxidant activity observed for these complexes is mainly attributed to the coordinated metal ion that modifies the overall activity as well as to the inherent antioxidant activity of the ligand; the presence of conjugated double bonds and the electron donating atoms being the properties of the ligands.

3.7.2. Antibacterial Activity

The novel metal complexes (L1Cu, L1Ni, L2Cu, L2Ni) were thoroughly evaluated for their antibacterial properties against four representative bacterial strains, namely Escherichia coli (Gram-negative), Pseudomonas aeruginosa (Gram-negative), Bacillus subtilis (Gram-positive), and *Staphylococcus aureus* (Gram-positive). Based on these results, which were sharply presented in quantitative form by measurement of

Table 5: Antioxidant activity (IC_{50} values in μg/mL) of the synthesized complexes and Ascorbic Acid control

Complex / Control	DPPH IC_{50} (μg/mL)
L1Cu	45.45 ± 0.45
L1Ni	55.56 ± 0.56
L2Cu	39.29 ± 0.54
L2Ni	51.32 ± 0.52
Ascorbic Acid	25.0±0.40

*Values are shown as mean ± SD (n = 3).

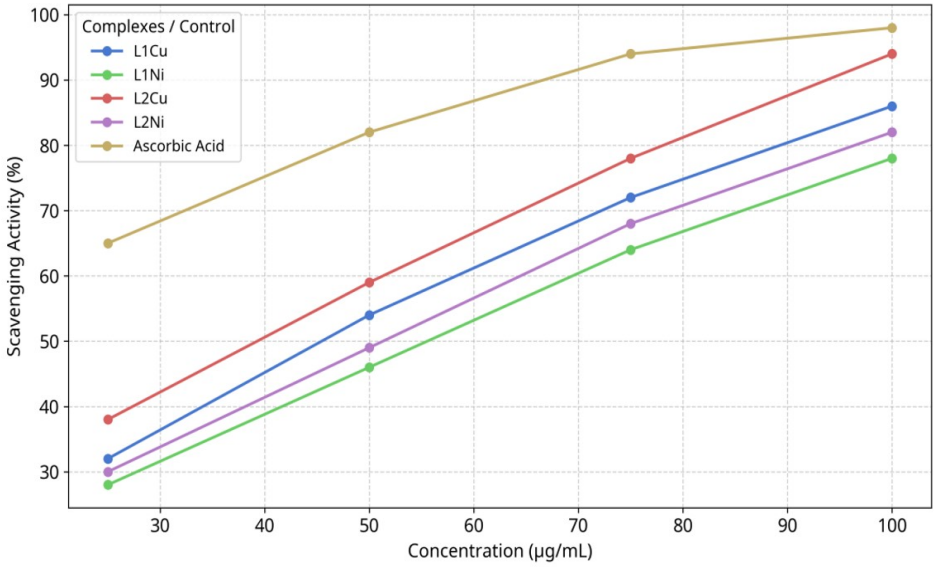


Figure 14: DPPH free radical scavenging activity curves of metal complexes and Ascorbic Acid at different concentrations, illustrating the relationship between concentration and scavenging percentage

inhibition zones with diameter, all the complexes proved to have some different antibacterial activity Table 6 & Figure 15. The free ligands (L1 and L2) were also screened for antibacterial activity as baseline to compare the activity of the metal complexes. The results were shown that free ligands were found to possess minimal antibacterial activity (4-8 mm) but were found to be effective for their metal complexes. The importance of the role metal coordination has on the enhancement of bioactivity of the synthesized compounds is highlighted by this baseline data. Notably, the consistently superior antibacterial activity, when compared to its nickel complexes (L1Ni and L2Ni), of the copper complexes (L1Cu and L2Cu) for all species of the bacteria tested. Interestingly the compound L2Cu was found to be the most effective antibacterial compound and exhibited the greatest inhibition zones against all bacterial strains.

Table 6: Antibacterial activity (Inhibition zone in mm) of the synthesized complexes

Complex	*S. aureus*	*B. subtilis*	*E. coli*	*P. aeruginosa*
L1	9±0.55	11±.82	11±0.52	10±0.72
L2	12±0.69	11±0.92	13±0.87	10±0.42
L1Cu	24±1.2	22±0.53	19±0.75	17±0.88
L1Ni	18±0.95	16±0.65	14±0.92	12±0.54
L2Cu	28±1.5	25±1.2	21±0.76	19±0.63
L2Ni	22±1.2	20±0,87	17±0.74	15±0.87

*Values are shown as mean ± SD (n = 3).

4. Discussion

Analyses of the physicochemical and biological features of the arsanilic-acid-derived relatively new type of organometallic compounds are key for the preparation of new therapeutic compounds. High purity and stability of the ligands (L1 and L2) and the metal complexes formed with the ligands were demonstrated from the synthesis and initial physical characterization results. The elemental analysis (CHN) results show excellent agreement between the experimental and the calculated as this perfectly matches the synthetic pathway followed (diazo transfer coupling), beside the achieved correct molecular formulas [17]. Moreover, the high decomposition temperatures of the complexes (L1Cu: > 360°C) showing a significant increase compared with their free ligands indicate a high degree of thermal stability induced by the coordination process, with the addition of a more solid framework based on the formation of strong coordinate covalent bonds [18].

Molar conductance values of the complexes in DMSO showed low values (13.24 to 16.50 $\Omega^{-1}\,cm^2\,mol^{-1}$) indicative of their predominant non-electrolytic nature in solution [19]. From this result it is indicated that the chloride ions are not free dissociated counter-ions but the locations of the chloride and solvent molecules in the co-ordination sphere needs to be confirmed by complete formulation and structural

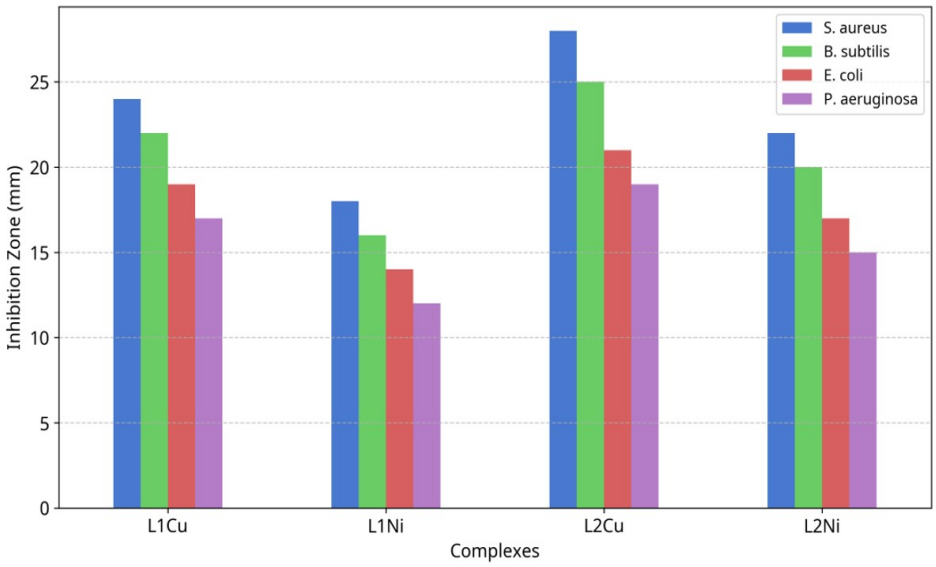


Figure 15: Comparison of antibacterial activity of different metal complexes, expressed as inhibition zone (mm) against four bacterial strains

analysis. It was found that the magnetic moment of both complexes Cu(II)L1 and Cu(II)L2 were 1.85 and 1.87 B.M, respectively. One unpaired electron exists within Cu(II) in these values, and are consistent with the proposed distorted square-planar coordination environments [20]. On the contrary, the magnetic moments of Ni(II) complexes, L2Ni and L1Ni, were found to be 3.29 and 3.31 B.M. respectively. As is found in Ni(II) ions with two unpaired electrons, these values are indicative of two octahedron coordination environments proposed [21]. From these observations and the combined magnetic, spectroscopic and conductivity information, the Cu(II) complexes are suggested to have distorted square-planar structure while Ni(II) complexes are suggested to have octahedral structure. Single crystal X-ray diffraction was not done on these assignments so the values are tentative.

The role of coordination played by various functional groups was confirmed by Fourier transform infrared (FT-IR) spectra. The azo group absorption bands (νN=N) are found to shift to lower frequencies in the complexes indicating the reduction in the bond order of the azo group as a result of withdrawal of the electrons towards the metal ion [22]. Furthermore, noticeable change in the band intensities in the carbonyl region (νC=O), and the appearance of additional bands in the lower frequency region associated with M-N and M-O bonds are indicative of the polydentate nature of the prepared ligands. Coordination is done through an azo nitrogen and the oxygen atoms of the carbonyl or hydroxyl groups, which are chemically stable five or six member rings [23, 24]. The formation of stable chelate rings joint is also provides multi-dentate stabilisation, contributing to the stability of the complex under several physiological conditions. These findings were supported by proton nuclear magnetic resonance (^{1}H-NMR) data, which showed that deprotonation occurs before metal binding, by disappearance of the signal related to the presence of the hydroxyl (-OH) proton (at 13.59-13.92 ppm in the free ligands). Small changes in the spectrum of the protons that can be used for aromatic resonance, such as those occurring upon coordination, describe changes in the electron environment of the molecule. In addition, by comparing the mass spectrometry results with theoretical values, the exact molecular weight of the compounds was confirmed and data for the molecular ion peak $[M]^+$ matched structural molecular weight calculations, minimizing the possibility of structural breakage or degradation when preparing the compounds [25]. There were characteristic electronic transitions observed in the optical spectra (UV-Vis); these played an important role in the study. Along with the $\pi \rightarrow \pi^*$ and n$\rightarrow\pi^*$ transitions that the ligand possesses, new bands were observed in the visible band in the complexes and d-d transitions are assigned to these bands of the metal, for Ni(II) and Cu(II) [26]. The ligand field strength as determined in these transitions closely mimics the results from magnetic measurements of square planar geometry (copper) and octahedral (nickel) [27]. Thermal analysis (TGA/DTA) also showed that the decomposition process occurs step-by-step until the formation of stable metal oxides, indicating that there are strong bindings between the metal and the ligand, as reported by Geobetsch et al. [28].

The results obtained by means of the thermal decomposition profiles obtained by TGA/DTA support the spectroscopic results and information about the coordination sphere. The initial mass loss is more indicative of the loss of lattice or solvent molecules than to the loss of coordinated water, the assignment of which is subject to confirmation from the molecular formula and complementary elemental analyses. In addition, the gradual deterioration of the organic component at high temperatures (200-500°C) indicates that the central metal ions have strong binding energies to the donor atoms (N, O) of the azo-hydrazone ligands. The weight remaining at high temperature agrees well with the calculated percentages, for the stable metal oxide residues CuO and NiO, and substantiates the proposed 1:2 stoichiometry and the structural integrity of the complex which have been synthesized.

In all biological assays free ligands L1 and L2 were included as baseline for assessing the possible synergistic effect of metal coordination. There is a good correlation between the free ligands and their metal complexes, supporting the principles of the Tweedy's Chelation Theory. Both free ligands (L1 and L2) showed weak antibacterial activity which might be explained by their high level of polarity, hindering them to penetrate into the lipophilic membrane of bacteria. The complexation of Cu(II) and Ni(II) lead to electron density delocalization over the whole chelate ring. Such partial donation of the positive charge of the metal by the metal atoms to the ligand donor atoms makes the resulting complexes very much lipophilic. Thus, the significant improvement in cell wall traversal efficiency of the metal complexes with regard to their intracellular target led to the noted synergistic improvement in the antibacterial activity. The high activity of the Cu (II) complexes (L1Cu and L2Cu) as compared with the Ni (II) complexes (L1Ni and L2Ni) indicates a profound effect of the redox property and coordination geometry of the metal center. Given that copper(II) is a redox-active ion, it can help to promote the production of reactive oxygen species (ROS) in target cells, which in turn can increase the oxidative stress. In addition, the square planar geometry of the copper

complexes is distorted so that it more readily interacts with the biological macromolecules than the more sterically hindered octahedral nickel complexes. The arsonic acid moiety (-AsO_3H_2) is also crucial as organoarsenic derivatives have been reported to affect the functions of mitochondria, especially in cancer cells, by interacting with the thiol groups in proteins. We speculate that the synergic effect of the bioactive ligand, derived from arsanilic acid, and the redox-active copper center leads to the strong therapeutic effects found in this study. The characteristic IR vibrations of the arsonic acid group (-AsO_3H_2) already indicate that this group is not coordinated, but will be available for biological interactions with cellular targets.

Following this, it was observed that the metal complexes had a significant superiority in inhibiting bacterial growth in comparison with the free ligands when used by themselves, during the transition to biological activity. Tweedy Chelation Theory can be used to explain this behavior; partial sharing of the positive charge of the metal ion with the donor groups make the compound more lipophilic, lowering its positive polarity [29]. Because of this improved lipid solubility, this compound is able to penetrate into the lipid-rich bacterial cell wall to interact with and neutralize crucial proteins and enzymes [30]. The L2Cu complex exhibited the largest inhibition zone, of 28 mm against *S. aureus*, which was believed that the larger inhibitory capacity was due to the combined action of the arsanil-derived ligand and the intrinsic copper toxicity of the complex [31].

DPPH radical-scavenging assay was done to assess the antioxidant activity of the complexes. The series of complexes exhibited the highest DPPH-scavenging activity as seen from a minimum IC_{50} values for L2Cu (39.29 μg/mL). This activity could be associated with the increase of the conjugation of the azo structure with the presence of electron-donating atoms that can help the stabilization of the radical [32]. Comparing the IC_{50} for both compounds, L2Cu was less effective with IC_{50} value was 39.29 ± 0.54 μg/mL compared to ascorbic acid which showed a lower value of IC_{50} of 25.0 ± 0.40 μg/mL in DPPH assay. Thus it may be concluded that, in vitro, the present results indicate a chemical radical-scavenging activity but such results should not be assumed to translate to clinical evidence for protection from oxidative stress [33]. In the present study is offered preliminary information regarding the antibacterial and DPPH-scavenging effects. In the current research, no anticancer assay, DNA-binding experiments nor apoptosis analysis was performed. Thus, potential anticancer benefits and DNA interactions are speculated and only to be confirmed by future in-depth studies of the genome- including DNA-binding assays, cytotoxicity, and apoptosis-related analyses.

5. Conclusion

The synthesis and characterization by elemental, spectroscopic, magnetic, thermal and mass-spectrometric methods are reported for two azo ligands and their Cu(II) and Ni(II) complexes, derived from arsanilic acid. From the available information distorted square-planar environments for the Cu(II) complexes and octahedral environments for the Ni(II) complexes were proposed. L2Cu was the most active amongst all the complexes studied and also showed the lowest IC_{50} value in DPPH radical scavenging. However under reported condition, its DPPH-scavenging activity was weaker than that of ascorbic acid. The activities observed are initial in-vitro results and need to be confirmed by mechanistic, cytotoxicity, DNA binding and toxicity studies.

Article Information

Data Availability: The datasets generated and/or analyzed during the current study are available from the corresponding author upon reasonable request.

Conflict of Interest: The author declares that there is no conflict of interest in this article.

Funding: No external funding was received for this study.

AI Use Disclosure: No generative artificial intelligence tools were used in the preparation of this manuscript.

References

[1] S. D. Oladipo and R. C. Luckay. New copper(II) and nickel(II) complexes derived from ONO-donor tridentate Schiff base ligands and 1-methyl imidazole as co ligand for their use as antidiabetes and antioxidants: Synthesis, crystal structures, DFT computational and in vitro studies. *Inorganica Chimica Acta*, 590:122977, 2026. URL https://doi.org/10.1016/j.ica.2025.122977.

[2] J. Ashraf and M. A. Riaz. Biological potential of copper complexes: A review. *Turkish Journal of Chemistry*, 46(3):595–623, 2022. URL https://doi.org/10.55730/1300-0527.3356.

[3] S. Baliyan, R. Mukherjee, A. Priyadarshini, A. Vibhuti, A. Gupta, and R. P. Pandey. Determination of antioxidants by DPPH radical scavenging activity and quantitative phytochemical analysis of Ficus religiosa. *Molecules*, 27(4):1326, 2022. URL https://doi.org/10.3390/molecules27041326.

[4] K. Mezgebe and E. Mulugeta. Synthesis and pharmacological activities of azo dye derivatives incorporating heterocyclic scaffolds: A review. *RSC Advances*, 12(40):25932–25946, 2022. URL https://doi.org/10.1039/D2RA04934A.

[5] S. S. S. Sandhu and G. K. Sandhu. Salts of metal ions with organic arsonic acids—I: Salts of phenylarsonic and o-arsanilic acids with cobalt(II), nickel(II), zinc(II) and cadmium(II). *Journal of Inorganic and Nuclear Chemistry*, 34(7):2249–2253, 1972. URL https://doi.org/10.1016/0022-1902(72)80158-1.

[6] R. Kılınçarslan, E. Erdem, and H. Kocaokutgen. Synthesis and spectral characterization of some new azo dyes and their metal complexes. *Transition Metal Chemistry*, 32(1):102–106, 2007. URL https://doi.org/10.1007/s11243-006-0134-x.

[7] B. Manjunatha, Y. D. Bodke, R. S. K. Jain, T. N. Lohith, and M. A. Sridhar. Novel isoxazolone based azo dyes: Synthesis, characterization, computational, solvatochromic UV-Vis absorption and biological studies. *Journal of Molecular Structure*, 1244: 130933, 2021. URL https://doi.org/10.1016/j.molstruc.2021.130933.

[8] P. S. Kalsi. *Spectroscopy of organic compounds*. New Age International Publishers, 2007.

[9] W. H. Mahmoud, M. M. Omar, and F. N. Sayed. Synthesis, spectral characterization, thermal, anticancer and antimicrobial studies of bidentate azo dye metal complexes. *Journal of Thermal Analysis and Calorimetry*, 124(2):1071–1089, 2016. URL https://doi.org/10.1007/s10973-015-5172-1.

[10] K. Yamjala, M. S. Nainar, and N. R. Ramisetti. Methods for the analysis of azo dyes employed in food industry—A review. *Food Chemistry*, 192 , URL:813–824, 2016. URL https://doi.org/10.1016/j.foodchem.2015.07.085.

[11] S. Benkhaya, S. M'rabet, and A. El Harfi. Classifications, properties, recent synthesis and applications of azo dyes. *Heliyon*, 6(1): e03271, 2020. URL https://doi.org/10.1016/j.heliyon.2020.e03271.

[12] N. M. Aljamali. Review in azo compounds and its biological activity. *Biochemistry & Analytical Biochemistry*, 4(2):169, 2015. URL https://doi.org/10.4172/2161-1009.1000169.

[13] D. P. Mishra, P. K. Sahu, B. Acharya, S. P. Mishra, and S. Bhati. A review of the synthesis and application of azo dyes and metal complexes for emerging antimicrobial therapies. *Results in Chemistry*, 10:101712, 2024. URL https://doi.org/10.1016/j.rechem.2024.101712.

[14] M. S. Masoud, S. S. Hemdan, and R. M. I. Elsamra. Synthesis, ligating properties, thermal behavior, computational and biological studies of some azo-transition metal complexes. *Journal of Inorganic and Organometallic Polymers and Materials*, 33(1):120–137, 2023. URL https://doi.org/10.1007/s10904-022-02483-x.

[15] S. Dudonné, X. Vitrac, P. Coutière, and M. Woillez. Comparative study of antioxidant properties and total phenolic content of 30 plant extracts of industrial interest using DPPH, ABTS, FRAP, SOD, and ORAC assays. *Journal of Agricultural and Food Chemistry*, 57(5): 1768–1774, 2009. URL https://doi.org/10.1021/jf803011r.

[16] Clinical and Laboratory Standards Institute. Performance standards for antimicrobial disk diffusion susceptibility tests. Clinical and Laboratory Standards Institute, 2018. 13^{th} Edition CLSI document M02.

[17] A. Frei, A. D. Verderosa, A. G. Elliott, J. Zuegg, and M. A. T. Blaskovich. Metals to combat antimicrobial resistance. *Nature Reviews Chemistry*, 7(3):202–224, 2023. URL https://doi.org/10.1038/s41570-023-00463-4.

[18] T. Aziz, H. A. Nasim, K. Ahmad, S. Parveen, M. M. Ahmad, H. Majeed, A. M. Galal, A. Rauf, and M. Ashfaq. Rational synthesis, biological screening of azo derivatives of chloro-phenylcarbonyl diazenyl hydroxy dipyrimidines/thioxotetrahydropyrimidines and their metal complexes. *Heliyon*, 9(1):e12492, 2023. URL https://doi.org/10.1016/j.heliyon.2022.e12492.

[19] N. N. Riaz, S. Iqbal, S. Amin, K. Ahmad, M. Atif, S. Muhammad, M. M. Ahmad, and M. Ashfaq. Rational synthesis of azo ligands and copper complexes: Insights into potential therapeutic agents. *Journal of Molecular Structure*, 1321:139705, 2025. URL https://doi.org/10.1016/j.molstruc.2024.139705.

[20] S. Kamali and S. Amani. Azo-imine based nickel(II), copper(II), and zinc(II) complexes: Synthesis, physicochemical and spectral investigations, quantum chemical calculations, molecular docking studies, and antibacterial investigations. *Inorganica Chimica Acta*, 563:121904, 2024. URL https://doi.org/10.1016/j.ica.2023.121904.

[21] I. V. Mañozca-Dosman, A. Aragón-Muriel, and D. Polo-Cerón. Antibacterial activity of metal complexes of Cu(II) and Ni(II) with the ligand 2-(phenylsubstituted) benzimidazole. *Scientia Pharmaceutica*, 93(2):22, 2025. URL https://doi.org/10.3390/scipharm93020022.

[22] N. T. A. Al-Rubaye and A. A. S. Al-Hamdani. Synthesizing, characterization of some metal ion complexes with new azo dye and studying antioxidant and anticancer (MCF-7). *Bulletin of the Chemical Society of Ethiopia*, 39(5):859–875, 2025. URL https://doi.org/10.4314/bcse.v39i5.5.

[23] A. Zavaroni, L. Rigamonti, F. Bisceglie, M. Carcelli, G. Pelosi, G. A. Gentilomi, D. Rogolino, and F. Bonvicini. Antimicrobial activity of copper(II), nickel(II) and zinc(II) complexes with semicarbazone and thiosemicarbazone ligands derived from substituted salicylaldehydes. *Molecules*, 30(11):2329, 2025. URL https://doi.org/10.3390/molecules30112329.

[24] N. Bayrak. Novel azanaphtoquinone compounds with aromatic amino moiety: Synthesis, structural characterization, and antimicrobial features. *Journal of Molecular Structure*, 1195:411–416, 2019. URL https://doi.org/10.1016/j.molstruc.2019.05.093.

[25] P. Marinova and M. Hristov. Synthesis and biological activity of novel complexes with anthranilic acid and its analogues. *Applied Sciences*, 13(16):9426, 2023. URL https://doi.org/10.3390/app13169426.

[26] A. A. Helaly, A. A. El-Bindary, and S. A. Elsayed. Synthesis and characterization of Co(II), Ni(II), Cu(II) and Zn(II) chelates: DFT calculations, molecular docking and biological applications. *Journal of Molecular Liquids*, 389:122831, 2023. URL https://doi.org/10.1016/j.molliq.2023.122831.

[27] T. Tahir, M. I. Shahzad, R. Tabassum, M. Rafiq, M. Ashfaq, M. Hassan, K. Kotwica-Mojzych, and M. Mojzych. Diaryl azo derivatives as anti-diabetic and antimicrobial agents: Synthesis, in vitro, kinetic and docking studies. *Journal of Enzyme Inhibition and Medicinal Chemistry*, 36(1):1508–1519, 2021. URL https://doi.org/10.1080/14756366.2021.1929949.

[28] S. Gozdas, M. Kose, V. McKee, M. Elmastas, I. Demirtas, and M. Kurtoglu. Crystal structures, electronic spectra and anticancer properties of new azo-azomethines and their nickel(II) and copper(II) chelates. *Journal of Molecular Structure*, 1304:137691, 2024. URL https://doi.org/10.1016/j.molstruc.2024.137691.

[29] K. J. Al-Adilee and A. S. Waheeb. Preparation, spectroscopic and anticancer studies of metal antibiotic chelation Ni(II), Cu(II) and Zn(II) 4,5-dimethyl thiazolylazo complexes. *Journal of Physics: Conference Series*, 1664(1):012057, 2020. URL https://doi.org/10.1088/1742-6596/1664/1/012057.

[30] P. Senthilraja and K. Kathiresan. In vitro cytotoxicity MTT assay in Vero, HepG2 and MCF-7 cell lines study of marine yeast. *Journal of Applied Pharmaceutical Science*, 5(3):80–84, 2015. URL https://doi.org/10.7324/JAPS.2015.50313.

[31] H. A. Abbas, K. K. Abbas, and A. M. H. A. Al-Ghaban. Magnetic MXene/g-C3N4 nanocatalyst for photocatalytic degradation of clindamycin contaminate in wastewater. *Results in Chemistry*, 13:101934, 2025. URL https://doi.org/10.1016/j.rechem.2024.101934.

[32] K. Ngece, V. Khwaza, A. M. Paca, and B. A. Aderibigbe. The antimicrobial efficacy of copper complexes: A review. *Antibiotics*, 14 (5):516, 2025. URL https://doi.org/10.3390/antibiotics14050516.

[33] A. C. Hangan, R. L. Lucaciu, A. Turza, L. Dican, B. Sevastre, E. Páll, L. S. Oprean, and G. Borodi. New copper complexes with antibacterial and cytotoxic activity. *International Journal of Molecular Sciences*, 24(18):13819, 2023. URL https://doi.org/10.3390/ijms241813819.